

Trajectory Optimization for Cellular-Connected UAVs with Disconnectivity Constraint

Eyuphan Bulut* and İsmail Güvenç†

*Dept. of Comp. Science, Virginia Commonwealth University, Richmond, VA 23284

†Dept. of Elec. and Comp. Engineering, North Carolina State University, Raleigh, NC 27607

Email: ebulut@vcu.edu, iguven@ncsu.edu

Abstract—The popularity of unmanned aerial vehicles (UAVs) has been increasing recently thanks to their enhanced functionalities and decreasing manufacturing costs. Many military and civilian applications involve UAVs for usecases/missions ranging from surveillance to search and rescue. However, despite their advantages, UAVs typically require near ubiquitous network connectivity for a successful fulfillment of their missions, which is a challenging task to achieve. In this paper, we study the trajectory optimization for cellular-connected UAVs with a disconnection duration constraint. That is, the UAV with the mission of flying from a start location to a final location needs to find a path during which it does not lose its cellular connection via one of the ground base stations (GBS) in the area more than a given time constraint. As the problem is difficult to be solved optimally, we propose a dynamic programming based approximate solution within polynomial time. In simulations, we show that the proposed approach can achieve close-to-optimal results with remarkably low computation costs and its accuracy could be increased by adding more granularity to the approximation.

Index Terms—Drones, dynamic programming, path planning, trajectory optimization, UAV networks.

I. INTRODUCTION

Recently, unmanned aerial vehicles (UAVs), also known as drones, have attracted extensive commercial and academic interest as they offer many advantages such as high mobility, low cost, and on-demand deployment. Even though there are barriers to ubiquitous use of UAVs such as compliance to flight regulations, UAVs are becoming more practical and affordable, and taking significant roles in our society. Today, use of UAVs range from hobbies (e.g., selfie taking [1], [2]) to transportation (Amazon delivery [3], [4]), communication (Facebook Aquila [5], Google Balloon [6]), surveillance for public safety [7], [8], agriculture [9], and construction [10]–[12]. With their large scale adoption, decreasing costs, and rapid technological advancements that add to their capabilities, UAVs offer a tremendous opportunity to revolutionize critical emergency applications such as search-and-rescue (SAR).

A major challenge for operating UAVs during a mission is path planning: the UAV trajectory needs to be carefully designed such that the application requirements are satisfied. For example, for time critical emergency applications that UAVs are involved in such as SAR, a mission trajectory that maintains a continuous communication with the ground base stations (GBSs) could be vital. While most of the commercial UAVs today use point-to-point communication with their

This work was supported in part by NSF award CNS-1647217.

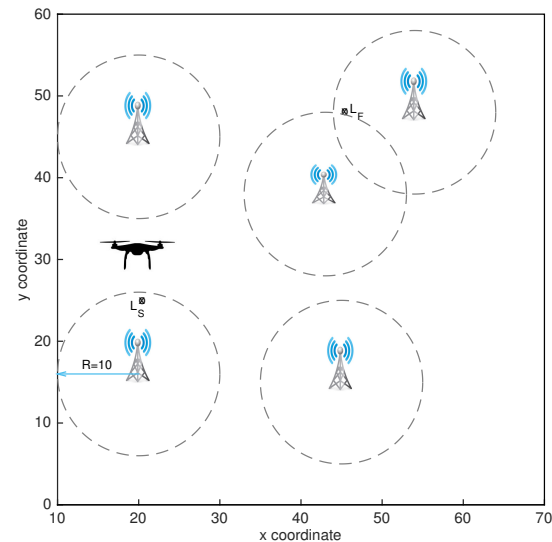


Fig. 1: Two dimensional view of an example scenario with 5 GBSs and a UAV that needs to travel from a starting location (L_S) to a final destination point (L_F). The ranges of GBSs are drawn considering the minimum distance required to achieve desired throughput between the UAV and the GBSs.

ground controllers over the unlicensed spectrum with limited performance, it has been shown that supporting UAVs using LTE networks [13]–[16] can extend the UAV operational range beyond LoS range.

Thanks to the investment done by various mobile operators, today, most of population areas worldwide are covered with cellular (e.g., LTE) connectivity yielding a high throughput, reliable and secure communication opportunity with another user at another location over the globe. With the upcoming 5G networks, this will reach higher performance and will help realizing more throughput hungry operations (e.g., streaming) and provide longer range of communication. However, due to the potential rural and unpopulated operation areas of UAVs, they may have partial or no cellular connectivity during their mission, especially when deployed at higher (e.g., millimeter-wave [17]) frequencies at 5G bands that face higher path loss and blocking effects compared to lower frequencies. This might result in interrupted communication with the operation base and might affect the success of the operation.

In this paper, we study the path planning of cellular-connected UAVs with disconnectivity constraint. An example

scenario is illustrated in Fig. 1, with several GBSs and a single UAV. The mission for the UAV is to fly from a start location, L_S , to a final location, L_F , without having more than a given disconnectivity duration continuously. As the coverage by all the GBSs in the figure does not make it possible to fly over a straight path between the given points, the optimum path should in any case include a disconnectivity time. Given a threshold for the allowed disconnectivity duration, the optimum path might be different. Moreover, even for the areas with existing possible paths that offer continuous connection, it may not be reasonable to unnecessarily prolong trajectory just for the sake of having continuous connectivity as this can increase the energy consumption. With some tolerance to disconnectivity, much better paths could be achieved. Note that such a disconnectivity threshold still has to be determined carefully without affecting the periodic data uploads/downloads required by the application as well as the control of the UAV.

We formulate the optimum trajectory finding problem for cellular-connected UAVs between a pair of points without exceeding a maximum disconnectivity duration. As the formulated problem is difficult to solve in general, we propose an approximated path based solution. To this end, we first define potential points using an overlay grid on the area for the movement of the UAV. Then, we formulate an efficient dynamic programming based solution under the given constraints. With the simulation results, we show that the proposed approximation path finding algorithm gives within 1% error of optimal results with a significantly reduced computation complexity. Moreover, its accuracy could be increased with more granularity added to the approximation.

The rest of the paper is organized as follows. We discuss the related work in Section II. In Section III, we provide the system model and describe the problem. Section IV presents the proposed model and the dynamic programming based approximated solution to the problem. Then, in Section V, we provide simulation results to validate the performance of the proposed design. Finally, we conclude the paper and provide future works in Section VI.

II. RELATED WORK

UAV trajectory design or path planning is essential for network performance optimization. Thus, it has been a major research area in the existing literature on UAVs. However, most of the studies are restricted to UAVs in the role of assisting cellular communication [18], in which the UAV provides cellular access to the other users by acting as a mobile relay or aerial base station. Several studies in that scenario have been conducted for a safe UAV navigation with various constraints such as interference management with other UAVs in the area [19]. In [20], joint optimization of communication power allocation and trajectory has been studied for mobile relaying systems to maximize the throughput. A distributed path planning algorithm is presented in [21] for multiple UAVs to deliver delay sensitive information to different nodes. An energy-efficient path planning is studied in [22]. In [23], a

mobility model that combines multiple constraints such as coverage, connectivity, and energy has also been studied for better path planning. An interesting approach is presented in [24] for trajectory optimization of UAV-enabled communication for best multi-casting performance.

Compared to the literature on UAV-aided wireless communication systems, there are a few works that have looked at the path planning for cellular-connected UAVs. In [25], a trajectory optimization for cellular-connected UAVs is investigated while maintaining its wireless connectivity with one of the GBSs at each time instant. However, the proposed solution only works if it is feasible to find a path with a continuous cellular connectivity which may not be true especially in wild and unpopulated areas. In [26], an interference-aware path planning for cellular-connected UAVs is studied and a deep reinforcement learning algorithm based on echo state network cells is proposed to achieve better wireless latency per UAV. Avoiding the low-coverage cellular communication during the flight of UAVs has also been studied in [27], with the concept of *holes-in-the-sky*. However, their focus is to define an accurate prediction model for aerial signal strength and let the UAV use it for better connectivity. In this paper, different than the previous work, we look at the path planning problem for cellular-connected UAVs for the rural areas where it may not be possible to find a continuously covered path or a limited disconnectivity might be tolerated to achieve better efficiency for the missions.

III. SYSTEM MODEL

We assume that there is a single cellular-connected UAV flying with a constant speed of V at a constant altitude of H meters (m). The set of GBSs are denoted by $\mathcal{G} = \{g_1, g_2, \dots, g_K\}$, with $|\mathcal{G}| = K$. The communication between the GBSs and the UAV is achieved through LTE or new generation 5G cellular communication technology. The mission of the UAV is to fly from a start location, L_S , to a final destination point, L_F , on an area of size N meters by M meters. The constraint for the UAV is, not to lose its cellular connection (i.e., maintaining a link with with one of the GBSs) more than τ_{\max} time units.

The location of i^{th} GBS, g_i , is denoted as (x_i, y_i, z_i) using a Cartesian coordinate system. For the sake of simplicity, we assume that all the GBSs have the same altitude, which is equal to H_G (i.e., $z_i = z_j = H_G \forall i, j \in [1, K]$). Furthermore, we denote the start location with $L_S = (x_S, y_S, z_S)$ and the end location with $L_F = (x_F, y_F, z_F)$, where $z_S = z_F = H$. As the UAV will be moving, we denote its location at time t with $(x(t), y(t), H)$, with $0 \leq t \leq T_{\max}$, where T_{\max} is the maximum flying time of the UAV at that constant speed V with its current battery capacity.

Each GBS and the UAV is assumed to be equipped with a single antenna with omni-directional unit gain. Moreover, similar to previous work [25], the channel between the UAV and a GBS is assumed to be dominated by the LoS link. Given the specifications of the GBSs, a range R is defined for minimum SNR needed for the communication between

the UAV and the GBSs. This could be computed using the following equation [25]:

$$R = \sqrt{\frac{\gamma_0}{S_{\min}} - (H - H_G)^2}, \quad (1)$$

where $\gamma_0 = \frac{P\beta_0}{\sigma^2}$ denotes the reference SNR, with P as the transmission power of each GBS, σ^2 as the noise power at the UAV receiver, and β_0 as the channel power gain at the reference distance of 1 m. S_{\min} above is the minimum required SNR value for the communication between the UAV and the GBSs in the application. We assume that the SNR at the receiver UAV shows the connectivity quality for the cellular-connected UAV communication.

The goal is to minimize the UAV trajectory distance, D , without staying out of range more than τ_{\max} time units continuously. Note that, since for the sake of simplicity we assume the speed of the UAV is constant, the distance traveled by the UAV for each time unit (e.g., seconds) will be the same. Thus, the minimum distance will also give the minimum mission travel time, without exceeding a continuous flight distance of d_{\max} that is out of the ranges of GBSs. Let $P(L_S, L_F) = \langle (x(0), y(0)), (x(1), y(1)), (x(2), y(2)), \dots, (x(T-2), y(T-2)), (x(T-1), y(T-1)), (x(T), y(T)) \rangle$ denote the path between the start and final locations that lasts T time units where $(x(i), y(i))$ denotes the horizontal position of the UAV at i^{th} time unit. Moreover, let $C_P = \langle c_0, c_1, c_2, \dots, c_{T-1}, c_T \rangle$ denote the set of binary values (e.g., 0 or 1) that indicate whether the locations at each time unit on path P is within R distance of at least one GBS or not. That is:

$$c_i = \begin{cases} 1, & \text{if } \exists g_k \in \mathcal{M} \text{ s.t. } \text{dist}_{(x(i), y(i))}^{(x_k, y_k)} \leq R, \\ 0, & \text{otherwise.} \end{cases}$$

where,

$$\text{dist}_{(x_1, y_1)}^{(x_2, y_2)} = \sqrt{(x_1 - x_2)^2 + (y_1 - y_2)^2 + (H - H_G)^2}.$$

The objective function can then be formulated as:

$$\min \quad T \quad (2)$$

$$\text{s.t.} \quad (x(0), y(0)) = (x_S, y_S) \quad (3)$$

$$(x(T), y(T)) = (x_F, y_F) \quad (4)$$

$$(\rho(t) - t - 1) \leq \tau_{\max}, \quad \forall t \in [0, T] \text{ w/ } c_t = 1, \quad (5)$$

where $\rho(t) = \arg \min_{\forall s > t} \{c_s = 1\}$. Here, (3) and (4) set the first and last points of the path as the starting and destination locations, respectively, and (5) ensures that there does not exist a continuous duration more than τ_{\max} without being covered by any GBS. As this formulated problem is difficult to be optimally solved, we propose a dynamic programming based approximate solution within a low complexity in the next section.

IV. PROPOSED DYNAMIC PROGRAMMING APPROACH

In this section, we present a dynamic programming based approximate optimum trajectory calculation for a cellular-connected UAV between a pair of locations. We first add a grid overlay on the area with the UAV and GBSs. The size of

each cell is set to 1 m by 1 m, thus, for example, an area with 1 km by 1 km is represented by a 1000 by 1000 grid overlay. Each point in the grid represents the potential locations of the UAV during its movement from start location to the final point.

Let $\mathcal{N}(i, j)$ denote the neighbor points of point (i, j) at the grid. That is:

$$\mathcal{N}(i, j) = \{(x, y) \mid \text{dist}_{(i, j)}^{(x, y)} \leq n_r \text{ and } (x, y) \neq (i, j)\}.$$

Here, n_r is the predefined neighbor range and defines the granularity of the algorithm together with the size of the each grid cell.

Moreover, let \mathcal{D}_{ij} denote the minimum trip distance to reach the grid point at (i, j) and \mathcal{I}_{ij} denote the interrupted cellular connection (i.e., disconnectivity) distance that the UAV has traveled just before reaching to the point (i, j) during this trip with minimum distance. Note that if the point (i, j) is already covered by a GBS, $\mathcal{I}_{ij} = 0$. On the other hand, it shows the distance traveled since the last covered point.

The minimum trip distance to point (i, j) has to satisfy the following equation due to the subproblem concept.

$$\begin{aligned} \mathcal{D}_{ij}(t+1) &= \min\{\mathcal{D}_{xy}(t) + \text{dist}_{(i, j)}^{(x, y)}\}, \\ &\quad \forall (x, y) \in \mathcal{N}(i, j) \text{ and} \\ &\quad \mathcal{I}_{xy}(t) + \text{dist}_{(i, j)}^{(x, y)} \leq d_{\max} \end{aligned} \quad (6)$$

That is, if the UAV can reach to point (i, j) from a neighbor point (x, y) without exceeding the limit for the disconnected duration and if it is less than the costs of the paths previously calculated, the new optimal path will be from that neighbor point. If the update in (6) is repeated with sufficient number of times, then the optimal path will be reached for the UAV under the given constraint. The number of such required iterations, \mathcal{X} , could be derived by:

$$\mathcal{X} = \frac{NM}{4R^2(n_r)^2} \quad (7)$$

This is because the GBSs could be distributed in a way that their coverage areas do not overlap and the only way to pass between them occurs only at the end and beginning of every other row. Thus, for example, the UAV may need to fly from east to west and back from west to east multiple times sweeping the entire area with such zigzags. Due to the design of the algorithm, as the update for the UAV location could occur with the maximum distance of n_r at every iteration, it can reduce the number of iterations needed. However, those neighbor based updates at every iteration will still be counted towards the algorithm's complexity. Note that (7) calculates the iterations needed for the worst possible case, however a smaller value could be calculated using the relative positioning of L_S and L_F with respect to the distribution of the GBSs.

In Algorithm 1, a pseudocode of the proposed dynamic programming approach for the optimal trajectory finding is presented. As the minimum distance to some points in some specific maps could be obtained after \mathcal{X} iterations at the latest, \mathcal{D} and \mathcal{I} arrays are created to store the status for each point at each iteration. Initially, for all points, \mathcal{D} and \mathcal{I} values are

Algorithm 1: Trajectory Finder w/ Dynamic Programming

```

1 for  $t = 1$  to  $\mathcal{X}$  do
2   for  $i = 0$  to  $N$  do
3     for  $j = 0$  to  $M$  do
4        $\mathcal{D}[i][j][t] = \infty$ 
5        $\mathcal{I}[i][j][t] = \infty$ 
6     end
7   end
8 end
9  $\mathcal{D}[x_S][y_S][0] = 0$ 
10  $\mathcal{I}[x_S][y_S][0] = 0$ 
11 for  $t = 1$  to  $\mathcal{X}$  do
12   for  $i = 0$  to  $N$  do
13     for  $j = 0$  to  $M$  do
14       for  $\forall p = (px, py) \in \mathcal{N}(i, j)$  do
15          $\Delta d = \text{dist}_{(i,j)}^{(px,py)}$ 
16         if  $\mathcal{D}[px][py][t-1] + \Delta d < \mathcal{D}[i][j][t]$  then
17           if  $(\mathcal{I}[px][py][t-1] + \Delta d \leq d_{\max}) \parallel$ 
18              $(\mathcal{C}[i][j] = 1)$  then
19              $\mathcal{D}[i][j][t] = \mathcal{D}[px][py][t-1] + \Delta d$ 
20              $\Pi[i][j] = (px, py)$ 
21             if  $\mathcal{C}[i][j] = 1$  then
22                $\mathcal{I}[i][j][t] = 0$ 
23             else
24                $\mathcal{I}[i][j][t] = \mathcal{I}[px][py][t-1] +$ 
25                  $\Delta \bar{d}$ 
26             end
27           end
28         end
29       end
30     end
31   end
32 end
33 return  $\mathcal{D}[x_F][y_F][\mathcal{X}-1]$ 

```

set to ∞ (lines 1-8). Then, since the UAV starts from the location L_S , the $\mathcal{D}(x_S, y_S)$ and $\mathcal{I}(x_S, y_S)$ is set to 0 for the start location (line 9-10). After this initial setup, the check (lines 16-17) for any update for each point is iterated \mathcal{X} times and the optimum path with the minimum possible distance (or travel time) is found (lines 11-31). At every iteration, once an update is done for a point, its updating neighbor point is also recorded in $\Pi[i][j]$ for finding the actual path (line 19). Note that, even though two consecutive points on a path are both covered by a GBS on the map, it is still possible that some small portion of the traveled line between these points could be uncovered. In order to improve the accuracy in that sense, an accurate uncovered distance, $\Delta \bar{d}$ (line 23), could be calculated by dividing the path into small parts and checking if each part is covered. However, such a check should be done only if there is an update needed not to increase the algorithm's complexity unnecessarily. Without that improvement, the complexity of the algorithm is $\mathcal{O}(\mathcal{X}NM)$, where \mathcal{O} shows the big-oh

Algorithm 2: Trajectory Readout

```

1  $curLoc = (x_F, y_F)$ 
2  $continue = true$ 
3 while  $continue$  do
4    $preLoc = \Pi[curLoc.x][curLoc.y]$ 
5   print  $preLoc$ 
6    $curLoc = preLoc$ 
7   if  $preLoc = (x_S, y_S)$  then
8      $cont = false$ 
9   end
10 end

```

notation.

Algorithm 1 only returns the minimum path distance under the given disconnectivity constraint. The actual path for the found path could be readout by Algorithm 2. As the neighbor location that updates a point on a trajectory with smallest possible distance is stored at $\Pi[i][j]$, the algorithm reads these values starting from the final location towards the start location.

V. SIMULATION RESULTS

In this section, simulation results to evaluate the performance of the proposed dynamic programming based trajectory finding algorithm for different deployments are presented. Specifically, we have generated two different maps with different number and distribution of GBSs over the area. In the first one shown in Fig. 2, 6 GBSs are deployed in a way that there is a possible path without interrupting the connectivity and the coverage areas of the some GBSs overlap with each other, providing shorter paths through their intersecting points. The second map is shown in Fig. 3. There are 9 GBSs deployed without any overlap. The start and final locations of the UAV is also selected in a way that the size of the path could potentially be more than the sum of sides of the area. This is to observe the need to run the outer loop of the algorithm with necessary number of iterations. Note that in both maps, we show the x and y coordinates with time units traveled. Table I shows the summary of the rest of the parameters and their corresponding values used for the simulations. We have taken some of these values from [25]. Under the given parameter settings, R can be derived as 10 time units, which is equal to 500 m.

TABLE I: Simulation settings.

	Map 1	Map 2
(N, M)	(70, 60)	(80, 60)
Number of GBSs	6	9
Starting location (L_S)	(25, 20)	(46, 46)
Final location (L_F)	(5, 5)	(75, 55)
H (height of UAV)	90 m	
H_G (height of GBSs)	12.5 m	
Reference SNR (at 1 m)	80 dB	
S_{\min}	26.02 dB	
V (speed of UAV)	50 m/s	
n_r (units)	3	

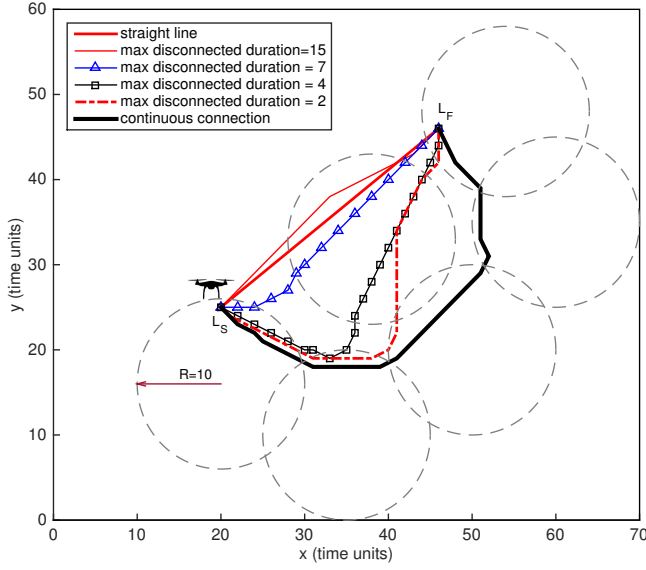


Fig. 2: Trajectories with different constraints on Map 1.

When we look at the results in Fig. 2, we first observe that the path with continuous connectivity requirement all the way to the destination is achieved through the intersection points (e.g., handover locations between neighbor GBSs) as also shown in [25]. However, due to the current granularity used in the algorithm it shows slight diversions which is less than 1%. Moreover, with a very high disconnectivity tolerance, the found trajectory is close to the straight line with a 1.1% difference. For the other tolerance levels in between these, a different path is obtained.

In Fig. 3, three different paths are plotted. Since the deployment of GBSs does not make it possible to have a path with continuous connectivity, we plot the one with minimum possible disconnectivity (i.e., 2 time units of travel). The path with that setting is a zigzag style path which requires multiple travels of the area from one side to the other. Thanks to the iteration count, \mathcal{X} , set appropriately, optimal path is obtained for such cases too. An interesting observation is, the simulation with maximum disconnection duration set to 12 time units generates a path where one GBS (i.e., the neighbor of the GBS with final location) is visited for a time unit only to break the current disconnectivity duration and the new disconnectivity period has started. Even though this is expected per design, it might be reasonable to set a minimum connectivity duration (e.g., $\bar{\tau}_{\min}$) needed to have necessary communication opportunity (e.g., for uploads of the data cumulated during disconnected duration) after a disconnectivity duration. To this end, the algorithm could be easily extended by setting another constraint similar to (5) such as:

$$(\lambda(t) - t - 1) \geq \bar{\tau}_{\min}, \forall t \in [0, T] \text{ with } c_t = 0, \quad (8)$$

where $\lambda(t) = \arg \min_{s > t} \{c_s = 0\}$.

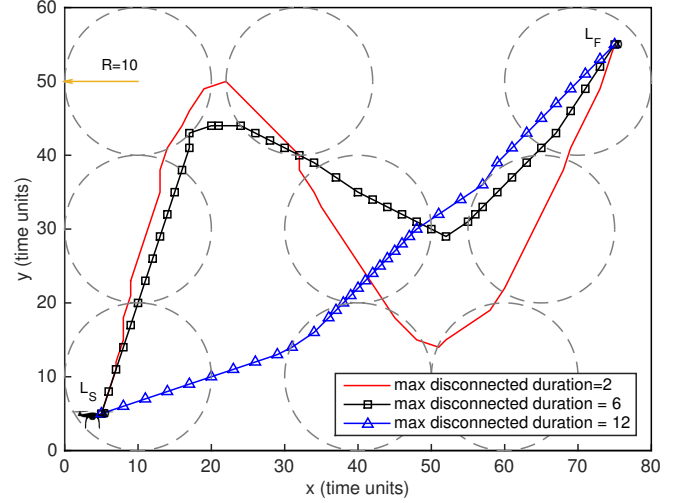


Fig. 3: Trajectories with different constraints on Map 2.

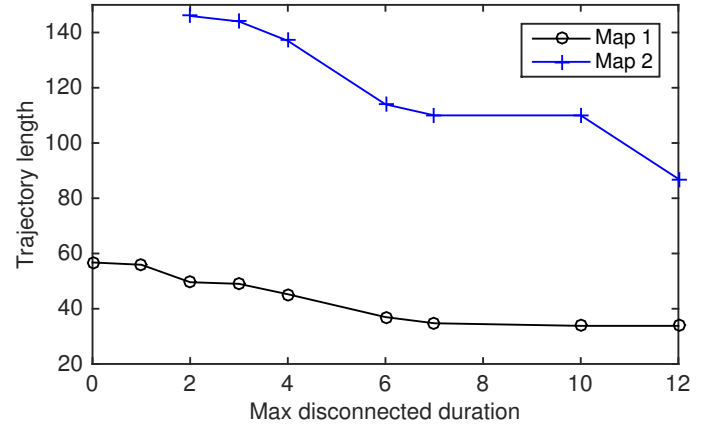


Fig. 4: The change in the length of the trajectory with different maximum disconnection time constraints.

In Fig. 4, the path lengths calculated under different maximum disconnection duration on the two maps are shown. Note that since there is no feasible path with d_{\max} set to 1 and 0 time units, corresponding lengths are not plotted. It is interesting to observe that the path lengths do not change for certain ranges of d_{\max} for both maps (e.g., from 7-10). This is because the deployment of GBSs in both maps does not offer any trajectory with smaller distance even though the limit is relaxed.

Finally, we plot the difference of the obtained path distances from the optimal results we found with exhaustive search. Fig. 5 shows these values for both maps. We observe that the proposed dynamic programming based approximated path finding algorithm achieves around 2% more path length, with $n_r = 3$, compared to the optimal paths with different constraints used. However, as it is shown in the figure, if we

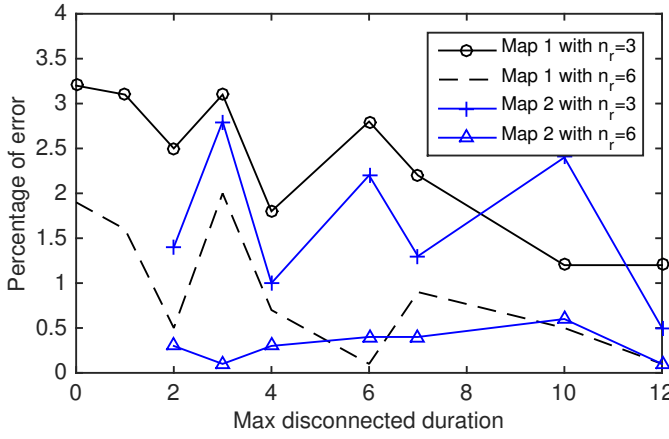


Fig. 5: The difference of obtained path distance from the optimal path.

start checking more neighbors at every iteration (e.g., $n_r = 6$), the difference could be decreased to less than 1%.

VI. CONCLUSION

In this paper, we investigate the trajectory optimization for cellular-connected UAVs under a continuous disconnection duration constraint. The UAV has the mission of flying from a pair of locations without losing its cellular connection with one of the ground base stations (GBS) more than a given time constraint. We formulated the problem and provided a dynamic programming based approximation solution within reduced complexity. Simulations results show that the proposed approach can achieve close-to-optimal results while having low computation costs. Moreover, its accuracy could be increased with more granularity added to the approximation. In our future work, we will extend the ideas here involving the battery capacity of the UAVs and try to optimize the mission completion times that require multiple trips [28]. We will also consider multiple UAV scenarios and DTN type communication [29] requirements (e.g., interconnectivity limit) between UAVs in determining the UAV trajectories.

REFERENCES

- [1] "Lily." [Online]. Available: <https://www.lily.camera>
- [2] S. Rosenbloom, "The selfie-drone: Invasion of the vacation snatchers," NY Times, August 2015. [Online]. Available: <http://www.nytimes.com/2015/09/06/travel/selfie-camera-drones.html>
- [3] Amazon Prime Air, "<http://www.amazon.com/b?node=8037720011>."
- [4] H. Menouar, I. Guvenc, K. Akkaya, A. S. Uluagac, A. Kadri, and A. Tuncer, "UAV-enabled intelligent transportation systems for the smart city: Applications and challenges," *IEEE Commun. Mag.*, vol. 55, no. 3, pp. 22–28, 2017.
- [5] Facebook Aquila Unmanned Aircraft Project at Connectivity Lab, "<https://info.internet.org/en/story/connectivity-lab/>."
- [6] Google: Loon Project, "<http://www.google.com/loon/>."
- [7] D. C. L. Kristen Boon, *The Domestic Use of Unmanned Aerial Vehicles*. Oxford University Press, 2014.
- [8] A. Kumbhar, I. Guvenc, S. Singh, and A. Tuncer, "Exploiting LTE-Advanced HetNets and FeICIC for UAV-assisted public safety communications," *IEEE Access*, vol. 6, pp. 783–796, 2018.

- [9] U. Weiss and P. Biber, "Plant detection and mapping for agricultural robots using a 3D LIDAR sensor," *Robotics and Autonomous Systems*, vol. 59, no. 5, pp. 265–273, 2011, special Issue ECMR 2009.
- [10] F. Caballero, L. Merino, J. Ferruz, and A. Ollero, "A visual odometer without 3D reconstruction for aerial vehicles. applications to building inspection," in *Proc. IEEE Int. Conf. Robotics and Automation (ICRA)*, 2005, pp. 4673–4678.
- [11] K. Alexis, G. Darivianakis, M. Burri, and R. Siegwart, "Aerial robotic contact-based inspection: planning and control," *Autonomous Robots*, pp. 1–25, 2015. [Online]. Available: <http://dx.doi.org/10.1007/s10514-015-9485-5>
- [12] A. Bircher, K. Alexis, M. Burri, P. Oettershagen, S. Omari, T. Mantel and R. Siegwart, "Structural inspection path planning via iterative viewpoint resampling with application to aerial robotics," in *Proc. IEEE Int. Conf. Robotics and Automation (ICRA)*, May 2015, pp. 6423–6430. [Online]. Available: <https://github.com/ethz-asl/StructuralInspectionPlanner>
- [13] B. Van Der Bergh, A. Chiumento, and S. Pollin, "LTE in the sky: trading off propagation benefits with interference costs for aerial nodes," *IEEE Commun. Mag.*, vol. 54, no. 5, pp. 44–50, 2016.
- [14] X. Lin, V. Jainanarayana, S. D. Muruganathan, S. Gao, H. Asplund, H.-L. Maattanen, M. Bergstrom, S. Euler, and Y.-P. E. Wang, "The Sky Is Not the Limit: LTE for Unmanned Aerial Vehicles," July 2017. [Online]. Available: <https://arxiv.org/abs/1707.07534>
- [15] Qualcomm Technologies, Inc. (2017, May.) LTE unmanned aircraft systems trial report. [Online]. Available: <https://www.qualcomm.com/documents/lte-unmanned-aircraft-systems-trial-report>
- [16] 3GPP TR-36.777, "Enhanced LTE support for aerial vehicles," Tech. Rep., 2018. [Online]. Available: <https://portal.3gpp.org/desktopmodules/Specifications/SpecificationDetails.aspx?specificationId=3231>
- [17] W. Khawaja, O. Ozdemir, and I. Guvenc, "UAV air-to-ground channel characterization for mmWave systems," in *Proc. IEEE Vehic. Technol. Conf. (VTC) Workshops*, Sep. 2017.
- [18] J. Lyu, Y. Zeng, and R. Zhang, "Cyclical multiple access in UAV-aided communications: A throughput-delay tradeoff," *IEEE Wireless Commun. Lett.*, vol. 5, no. 6, pp. 600–603, 2016.
- [19] C. Zheng, L. Li, F. Xu, F. Sun, and M. Ding, "Evolutionary route planner for unmanned air vehicles," *IEEE Trans. Robotics*, vol. 21, no. 4, pp. 609–620, 2005.
- [20] Y. Zeng, R. Zhang, and T. J. Lim, "Throughput maximization for UAV-enabled mobile relaying systems," *IEEE Trans. Commun.*, vol. 64, no. 12, pp. 4983–4996, 2016.
- [21] J. Yoon, Y. Jin, N. Batsoyol, and H. Lee, "Adaptive path planning of UAVs for delivering delay-sensitive information to ad-hoc nodes," in *Proc. IEEE Wireless Commun. Netw. Conf. (WCNC)*, 2017, pp. 1–6.
- [22] Y. Zeng and R. Zhang, "Energy-efficient UAV communication with trajectory optimization," *IEEE Trans. Wireless Commun.*, vol. 16, no. 6, pp. 3747–3760, 2017.
- [23] M.-A. Messous, S.-M. Senouci, and H. Sedjelmaci, "Network connectivity and area coverage for UAV fleet mobility model with energy constraint," in *Proc. IEEE Wireless Commun. Netw. Conf. (WCNC)*, 2016, pp. 1–6.
- [24] Y. Zeng, X. Xu, and R. Zhang, "Trajectory optimization for completion time minimization in UAV-enabled multicasting," *IEEE Trans. Wireless Commun.*, Early Access.
- [25] S. Zhang, Y. Zeng, and R. Zhang, "Cellular-enabled UAV communication: Trajectory optimization under connectivity constraint," *arXiv preprint arXiv:1710.11619*, Oct. 2017.
- [26] U. Challita, W. Saad, and C. Bettstetter, "Deep reinforcement learning for interference-aware path planning of cellular-connected UAVs," in *Proc. IEEE Int. Conf. Commun. (ICC)*, May 2018.
- [27] E. Teng, J. D. Falcão, and B. Iannucci, "Holes-in-the-sky: A field study on cellular-connected UAS," in *Proc. Int. Conf. Unmanned Aircraft Systems (ICUAS)*, 2017, pp. 1165–1174.
- [28] K. Dorling, J. Heinrichs, G. G. Messier, and S. Magierowski, "Vehicle routing problems for drone delivery," *IEEE Transactions on Systems, Man, and Cybernetics: Systems*, vol. 47, no. 1, pp. 70–85, 2017.
- [29] E. Bulut, S. C. Geyik, and B. K. Szymanski, "Utilizing correlated node mobility for efficient DTN routing," *Pervasive and Mobile Computing*, vol. 13, pp. 150–163, 2014.